Underground renewal time and mixing of the main mineral waters of Tunisia: A multi-tracer study

Philippe Jean-Baptiste, Elise Fourré, Elyès Gaubi, B. Minster, Luc Aquilina,
Thierry Labasque, J.L. Michelot, Marc Massault, Abdallah Ben Mammou

Underground renewal time and mixing of the main mineral waters of Tunisia : a multi-tracer study

P. Jean-Baptiste[1], E. Fourré[1], E. Gaubi[2], B. Minster[1], L. Aquilina[3], T. Labasque[3], J.L. Michelot[4], M. Massault[4], A. Ben Mammou[2]

[1]*LSCE, CNRS-CEA-UVSQ, Centre de Saclay, F-91191, Gif-sur-Yvette, France*
[2]*Laboratoire Ressources Minérales et Environnement, Univ. Tunis El-Manar, Tunisia*
[3]*CAREN, Géosciences Rennes, UMR 6118, CNRS-University of Rennes 1, POB 74205, F-35042, Rennes cedex, France.*
[4]*IDES, UMR 8148, CNRS-University of Paris 11, F-91405, Orsay, France.*

Abstract.

Bottled waters are increasingly popular in Tunisia. Most of them come from groundwaters, thus raising the question of the long-term availability of the mineral groundwater resources. Water collected from production springs or wells of eleven mineral waters of Tunisia among the main commercial brands were analyzed for tritium (^{3}H), helium-3, SF_6, CFCs and carbon-14. Tracer-tracer plots indicate that all of the groundwaters of our data set are a mixture of modern rainwater with older groundwater flow waters that are beyond the time-scale of the transient tracers. ^{14}C data suggest that the age of these old waters, which constitute the main water reservoir, is of the order of radiocarbon half-life or more. Most of the studied sites have groundwater renewal times in the range 50-150 years. For the sites where tracer concentrations are the most diluted by old waters, this value logically increase to several centuries.

1. Introduction

The rapid increase in bottled mineral groundwater production in Tunisia needed to meet consumer demand (110 millions bottles in 1995 and 1.04 billion bottles in 2015 – Office du thermalisme at *www.thermalisme.nat.tn*) raises the question of the long-term sustainability of this economic sector.

Renewal time of groundwater, which is clearly related to the ratio of the storage volume to the recharge rate, is an important notion regarding vulnerability and sustainability of groundwater resources. Numerical models of groundwater flow can describe accurately the hydrodynamic functioning of a given aquifer, and therefore can give stackeholders and the mineral water industry management important indications to prevent pollution and/or overexploitation of the water resource. However, they require detailed information (e.g. boundary conditions, hydraulic conductivity, porosity, etc...) which are usually not available. As an alternative, the analysis of atmospheric transient tracer concentrations in groundwaters can provide important basic information on their residence time and mixing.

As a development arising from tritium, which can be used as a transient tracer as a result of ^{3}H injection into the atmosphere from the atmospheric testing of nuclear devices in the 50's and early 60's, the ^{3}H-^{3}He dating method offers a direct measure for the time since groundwater had its last gas exchange with the atmosphere. The ^{3}H-^{3}He pair is of particular interest because tritium and its daughter helium-3 are assumed to be fully conservative tracers, and also because the ^{3}H-^{3}He radioactive clock only relies on the in-situ ^{3}H/^{3}He ratio. Hence, it is independent of the history of tritium input to the aquifer (Schlosser et al., 1988, 1989; Poreda et al., 1988; Solomon et al., 1991, 1993; Stute et al., 1997).

55 Like tritium, ^{14}C was also a by-product of atmospheric nuclear tests. Hence, the

56 resultant transient spike in atmospheric $^{14}CO_2$ can also be used as a transient tracer

57 (Stewart, 2012; Baudron et al., 2013).

58 The CFCs and SF_6 methods are based on the direct comparison of the

59 groundwater tracer concentration with the concentration of these tracers in the

60 atmosphere, and hence in groundwater recharge. Because their atmospheric

61 concentration has changed through time, this provides the basis for travel time

62 determination (Thompson and Hayes, 1979; Cook and Solomon, 1995; Busenberg

63 and Plummer, 1992, 2000; Goody et al., 2006; Darling et al., 2012).

64 Each tracer has its own atmospheric input function and each tracer method relies

65 on its own specific set of assumptions and caveats. There are significant differences

66 in the reliability of the derived tracer ages. Some caveats are the result of

67 hydrogeology. For CFCs and ^{14}C additional uncertainties of the infiltration conditions

68 influence the resulting ages.Therefore the combination of several tracer methods in

69 parallel is highly preferable to the use of a single method (Szabo et al., 1996; Beyerle

70 et al., 1999; Plummer et al., 2001; Corcho Alvarado et al., 2005, 2007; Massmann et

71 al., 2008; Solomon et al., 2010; Mayer et al., 2014; Kralik et al., 2014; Delbart et al.,

72 2014; Battle-Aguilar et al., 2017). Ideally measured tracer concentrations in a

73 groundwater can be matched simply to a particular year of recharge. However, this

74 requires that the groundwater moves as a result of simple piston flow, that is along

75 parallel flowlines from recharge to discharge. In reality, groundwaters are often a

76 mixture of water of different ages due to the complexity of the hydrogeological

77 network and/or the internal structure of the aquifer. One basic way of resolving flow

78 processes is to plot one tracer versus another (see for instance Figure 3 in Darling et

79 al., 2012). On these plots, simple piston flow and binary mixing between young

80 recharge waters and old tracer-free waters are opposite extremes of groundwater

81 behaviour. In most cases however, groundwater flow may be more complicated and

82 one must test a variety of modeled reservoirs connected to each other serially or in

83 parallel with or without dead volumes, cross flow in between or bypass flow (see

84 Ozyurt and Bayari, 2003 and references therein).

85   Here we report the application of such a multi-tracer approach to a suite of

86 mineral waters of Northern and Central Tunisia among the main commercial brands.

87 The region is characterized by a semi-arid climate with mild wet winters and hot dry

88 summers (monthly average temperatures vary from 10±1°C in January to 28±2°C in

89 August), and relatively low annual rainfall in the range 300 mm – 600 mm. For this

90 study, we selected eleven bottled water production sites (Table 1), exploiting local

91 aquifers nested in karstified limestone and/or sandstone formations (see Appendix

92 A). Very little is known by the operators concerning the actual extent of their mineral

93 groundwater resources and the sustainability of their business. Comparison of

94 mineral water withdrawal rates and recharge rates estimated from precipitation

95 figures and catchments' surface area shows that the rate of water withdrawal

96 exceeds the present-day recharge rate. This overexploitation of the local mineral

97 groundwater reservoirs may have serious implications in term of water quality and

98 economic consequences for the mineral water industry. Note that the issue of

99 groundwater overexploitation in Tunisia is not restricted to mineral waters: Tunisia,

100 being a semi-arid to arid country, is facing water shortage of increasing severity as a

101 result of population growth, rising living standards and increasing water consumption

102 by the agricultural sector (Frija et al., 2014)

103　　　The present work aims at exploring the potential of the selected suite of transient

104　tracers (tritium/helium-3, SF_6, CFCs and radiocarbon) to gain insight into the

105　hydrogeological characterization of these different water reservoirs.

106

107　**1. Sample collection and analytical methods**

108

109　　　The sampled sites are shown in Fig. 1, and their main characteristics (climatic

110　conditions, elevation, …) are summarized in Table 1. Groundwaters were analyzed

111　for $^{18}O/^{16}O$, D/H, ^3H, ^3He, ^4He, ^{20}Ne, CFCs (F-11, F-12, F-113), SF_6. and ^{14}C. Apart

112　from Marwa-2009 which shows a high neon supersaturation (see below), the

113　samples were taken at the water extraction point (at the well-head for pumped waters

114　and at the capture point for natural springs) so that contact of the water with the

115　atmosphere can be excluded. With the exception of a few tritium/helium and ^{14}C

116　samples taken in October 2009, all the water samples were collected in

117　September/October 2010.

118　　　CFCs and SF_6 samples were collected in air tight stainless steel cells of 30 and

119　500 ml respectively and were analyzed at the University of Rennes (Labasque et al.,

120　2006; Ayraud et al., 2008). The CFC and SF_6 concentrations were determined by

121　Purge and Trap (PT) extraction and analysed with a gas chromatograph equipped

122　with an electron capture detector (GC/ECD). The uncertainty is 3% for water

123　equilibrated with the present-day atmosphere for CFC and 5% for SF_6 (see Table 2).

124　　　Noble gas samples (He, Ne) were collected using standard refrigeration grade

125　3/8" copper tubes equipped with metal clamps at both ends. ^3H samples were

126　collected in 500 ml pyrex bottle, baked at 75°C and pre-filled with argon. The tritium

127　and noble gas isotopic analyses (^3He, ^4He, ^{20}Ne) were carried out at LSCE (CEA-

128   Saclay) with a MAP-215 mass spectrometer using standard procedures. Helium and

129   neon dissolved in the water samples were first extracted under vacuum into sealed

130   glass tubes. The accuracy is ±0.8% for helium and neon concentrations, and ± 0.4%

131   for the ^{3}He/^{4}He ratio. Water for tritium determination was degassed and stored during

132   9 to 12 months to allow for ^{3}He ingrowth. Uncertainty on tritium determination is given

133   in Table 2. Technical details concerning laboratory treatments and analytical

134   methods are available in Jean-Baptiste et al., 1992, 2010.

135   Carbon-14 samples were taken in 500 ml stainless steel cells and analyzed by

136   accelerator mass spectrometry at the French Radiocarbon National facility (CEA-

137   Saclay), with an accuracy between ±0.1 pmC and ± 0.2 pmC (see Table 2). Delta ^{13}C

138   was measured by IRMS at Paris-Sud University, with an accuracy of ± 0.1 ‰.

139   Water for stable isotope analysis was collected in 15 ml glass bottles. Deuterium

140   and oxygen-18 were analysed at LSCE (CEA-Saclay) by laser spectrometry.

141   Uncertainties are ± 0.15 ‰ and ± 0.7 ‰ for oxygen-18 and deuterium respectively.

142

143   **3. Results**

144

145   Analytical results are shown in Table 2 . Stable isotopes are between $-50.5‰$

146   and $-31.6‰$ for D/H and between -7.66 and -5.10 for $^{18}O/^{16}O$, respectively. The

147   lowest values correspond to the El Kef region and reflect the altitude effect of this

148   more elevated area (altitude > 850 m – see Table 1) on the water isotopes

149   composition of rainwaters (Ambach et al., 1968; Siegenthaler and Oeschger, 1980).

150   The results are consistent with precipitation isotopic data for northern and central

151   Tunisia represented by the Tunis and Sfax Local Meteoric Water Lines (Fig. 2),

152 indicating that the rainfall contributing to the recharge did not undergo any significant

153 evaporation before infiltration.

154   All waters are tagged to various degree with environmental tracers of the post-

155 1950 era (Table 1). In spite of this, all carbon-14 values (range : 2.2 to 68.7 pmC) are

156 well below the natural modern pre-nuclear value of 100 pmC. The lowest value

157 corresponds to the carbo-gaseous waters of Ain Garci ($[HCO_3]$ = 19.8 mmol/l), clearly

158 showing the influence of the ^{14}C dilution by dead carbon on the ^{14}C result. $\delta^{13}C_{TDIC}$

159 data were used to correct measured ^{14}C activities for dead carbon dilution due to

160 bicarbonate formation during the reaction between carbonic acid originating from soil

161 CO_2 and carbonate minerals (Clark and Fritz, 1997; Han and Plummer, 2016). For

162 this correction, the initial $\delta^{13}C$ value in groundwater recharge prior to leaving the

163 water-soil gas interaction zone is set to –12 ‰ (Clark and Fritz, 1997; Fourré et al.,

164 2011) and the $\delta^{13}C$ of the marine carbonate limestone formations (see Appendix A) is

165 assumed to be 0 ‰ (Clark and Fritz, 1997).

166   Neon excess relative to solubility equilibrium at the recharge temperature and

167 elevation ranges from –0.4% to 50.1% (mean value of 21.4%), with the exception of

168 Marwa which show a very large excess in 2009 (230%). This large anomaly, which is

169 confirmed by the analysis of a backup sample, is not seen in 2010 (26.6%). The most

170 probable explanation for the difference between 2009 and 2010 is the sampling

171 location : inside the bottling building in 2009 and at the well head in 2010. The neon

172 data are used to correct all tracer gas concentrations (^3He, ^4He, CFCs and SF_6) for

173 excess air (Aeschbach-Hertig et al., 1999) prior to age calculations and tracer

174 comparisons. In addition, all tracer concentrations are normalized to sea-level

175 pressure and a common temperature of 15°C to allow the comparison of all sites.

176   CFCs and SF$_6$ ages were determined from the direct comparison of the

177   groundwater tracer concentration with the time-dependent concentration of the tracer

178   in the groundwater recharge.

179   The ^{3}H/^{3}He age τ is defined as $\tau = \lambda^{-1} Ln(1+^3He_{tri}/^3H)$, where λ is the decay

180   constant of tritium and ^{3}H the measured tritium concentration. It is usually expressed

181   in tritium units (TU) : 1 TU corresponds to a ^{3}H/H ratio of 10^{-18}. $^3He_{tri}$ is the fraction of

182   the total ^{3}He that is produced by ^{3}H decay, i.e. the difference between the measured

183   concentration $^3He_{meas}$ and the concentrations of other ^{3}He components : $^3He_{atm}$ of

184   atmospheric origin, and $^3He_{ter}$, the terrigenic component : $^3He_{tri} = (^3He_{meas}-^3He_{atm}-$

185    $^3He_{ter})$. $^3He_{atm}$ and $^3He_{ter}$ are deduced from the measured concentrations of helium

186   and neon. A terrigenic ratio $^3He_{ter}/^4He_{ter}$ of 2×10^{-8} typical isotope ratio for radiogenic

187   helium production in rocks was used, according to the work of Fourré et al. 2011

188   which shows the absence of mantle helium in the studied area (except for Ain Garci –

189   see below). Note that $^3He_{ter}$ is very small, therefore $^3He_{tri}$ is relatively insensitive to the

190   value of this terrigenic ^{3}He/^{4}He ratio.

191   Tracer ages are reported in Table 2 and Figure 3. (Fig. 3). SF$_6$ ages are younger

192   and F-11 ages older than ^{3}H/^{3}He, F-12 and F-113 ages, possibly due to in-situ

193   terrigenic SF$_6$ production and F-11 breakdown (see section 4 below). For Ain Garci,

194   ^{3}H-^{3}He dating was problematic due to the presence of mantle ^{3}He

195   (^{3}He/^{4}He = $2.4 \times$ Ra – see Fourré et al., 2011). ^{3}H/^{3}He, F-12 and F-113 ages range

196   from 10 to 58 years but tracer ages show substantial discrepancies. Age calculations

197   assume that groundwater moves along independent flowlines analogous to pipes

198   (piston flow). However, tracer-tracer plots (see section 4 below) indicate that the

199   groundwaters are a mixture of modern waters withwith older (tracer-free) waters.

200   Therefore, the piston flow conditions are not valid here and under these conditions it

201 is not possible to assign ages to tracer concentrations. Therefore tracer ages

202 reported here are not true ages but "apparent" ages (Suckow, 2014). Actual tracer

203 concentrations are modified by this mixing which, in turn, variously affects tracer

204 ages, thus explaining the substantial discrepancies among tracers.

205

206 **4. Discussion**

207

208 Figure 4a displays the mean annual atmospheric concentrations of CFCs, SF_6

209 and ^{14}C as a function of time for the northern hemisphere. For tritium, the past history

210 of its concentration in precipitation in Tunisia was constructed using all historical

211 measurements from Central Mediterranean stations in the IAEA Global Network of

212 Isotopes in Precipitation database (at https://nucleus.iaea.org/wiser/gnip.php),

213 including the times-series of tritium in rainwater for Tunis and Sfax (Fig. 4b). Tunis

214 data agree with Central Mediterranean IAEA stations between 1970-1980 and then

215 seems to be overestimated, possibly due to data quality problems (some

216 contamination or analytical problems may be suspected). Sfax is on the lower side of

217 the IAEA central Mediterranean dataset, which is consistent with its southern

218 location. C-14 and tritium data are averaged using a polynomial function. The curves

219 in Figure 4a and 4b provide the basis for model calculations of the theoretical

220 relationships between the concentrations of the different transient tracers in

221 groundwater under various mixing assumptions.

222 Figure 5 compares the groundwater concentrations of F-11, F-12, F-113 and SF_6

223 for all groundwaters with the piston flow (PF) model, i.e. along tubular flow lines from

224 recharge to discharge with no mixing of the flow lines. Each curve (in black)

225 represents the relationship between a given tracer pair for recharge dates going back

226   in time from the sampling date (2010) to the pre-1950s years corresponding to

227   waters beyond the time-scale of the transient tracers. As a variante to this simple

228   piston flow model, we have also calculated the tracer-tracer relationships (blue

229   curves) for the PF model with a typical dispersion coefficient of 10^{-4} cm^2/sec along

230   the direction of the flow (PF+DIS). Figure 5 shows that at all sites the groundwater

231   concentrations disagree with both models and are better explained (dotted line) by a

232   simple binary mixing (BM) between "modern" waters (upper right corner) and "old"

233   tracer free waters (lower left corner). The PF and BM curves define the region that

234   should contain all tracer data if no additional process other than mixing affects the

235   tracer concentration (permitted region). In Figure 5b and 5c, most SF$_6$ and F-11

236   concentrations are somewhat outside the permitted region. As already noted above

237   when comparing the tracer ages (section 3), this indicates a small but significant

238   additional SF$_6$ component likely due to in-situ production (Harnisch and Eisenhauer,

239   1998; Busenberg anf Plummer, 2000; Deeds et al., 2008; Lapworth et al., 2015) as

240   well as some F-11 in-situ degradation (Oster et al., 1996; Shapiro et al., 1997;

241   Höhener et al., 2003).

242   This mixing trend defined by CFC tracer plots is also apparent on the tritium-F12

243   and tritium-radiocarbon diagrams (Fig. 6a and 6b). This latter diagram also suggests

244   that, for the various studied sites, the old water ^{14}C endmember is in the range 5 –

245   50 pmC, corresponding to radiocarbon ages between one and four radiocarbon half-

246   lifes (approximately 5000 to 20000 years). Radiogenic ^{4}He was plotted against these

247   radiocarbon ages (not shown) since one would expect radiogenic ^{4}He coming with

248   the old water. However, as already noticed in the above Results section, for all the

249   sites ^{3}He$_{ter}$ and ^{4}He$_{ter}$ are very small and do not provide any clear evidence of a

250   correlation with ^{14}C ages. This is probably because the old waters are too shallow to

251   pick-up significant crustal helium.

252   The fraction of old water present at each site, estimated from the F113 - F12 or

253   tritium - F12 diagrams, is shown in Fig. 7.

254   Qualitatively, one may say that this factor of dilution by the old waters is an

255   indication of size of the reservoir, and therefore of the sustainability of groundwater

256   resource. More quantitatively, the evolution of the tracer concentration C_n at year n

257   (for a well-mixed deep reservoir) can be deduced from the tracer concentration C_{n-1}

258   at year n-1 by writing the following tracer balance equation:

259                     $AH_n\, C_n = AH_{n-1}\, C_{n-1} + [A\, r\, (C_{surf})_n - A\, w\, C_{n-1}]\, \Delta t$ (1)

260   where Δt equals 1 year, r (in m/year) is the water recharge rate and w (in m/year) is

261   the withdrawal rate (both natural and anthropic). A (in m^2) is the surface area of the

262   recharge zone, (AH_n) and (AH_{n-1}) are the volume of groundwater at year n and n-1 (in

263   m^3) and $(C_{surf})_n$ is the tracer concentration in the recharge water of the year n.

264   In a similar way, the time-evolution of the volume of groundwater obeys the

265   following equation:

266                      $AH_n = AH_{n-1} + (A\, r - A\, w)\, \Delta t$ (2)

267   If one introduces the renewal time τ_n of the groundwater defined by $\tau_n = H_n/r$,

268   equations (1) and (2) can be rewritten as follows :

269                 $C_n\, \tau_n = C_{n-1}\, \tau_{n-1} + \Delta t\, [(C_{surf})_n - C_{n-1}\, w/r]$ (1')

270                       $\tau_n = \tau_{n-1} + \Delta t\, (1 - w/r)$ (2')

271   Note that for tritium, a radioactive decay is applied to the concentrations every year

272   (not shown in the above equations).

273   The concentration C_{2010} of each tracer at the year of sampling (2010) is

274   determined by solving equations (1') and (2') as a function of the initial renewal time

275   τ_{init} of the undisturbed reservoir (before the commissioning of the bottling plant) for

276   various w/r. The value of w/r, which is not known precisely, is assumed equal to 1 in

277   natural conditions. For all the sites where groundwater is pumped from a well,

278   different values of w/r between 1 and 10 are tested. Since C_{2010} must be equal to the

279   measured concentration, a value of τ_{init} can be determined for each tracer.

280   Calculations start in 1950 for CFC's with an initial concentration set to zero. For

281   tritium, an additional spin-up phase going from 1900 to 1950 is necessary to allow for

282   the establishment of the natural concentration in the groundwater reservoir. Table 3

283   displays the value of the renewal time at each site calculated for each tracer for w/r=1

284   and w/r=10. One can see that the impact of the value chosen for w/r remains limited.

285   This unexpected result is due to the fact that tracer infiltration started in the 1950's,

286   that is well before the commissioning of most of the sites (see Table 1); as a

287   consequence, because of the small withdrawal time compared to the tracer infiltration

288   history, the influence of the withdrawal rate has not enough time to really make a

289   strong difference. Tritium-based renewal times are systematically higher than those

290   of F-12 and F-113. For the majority of the studied sites, renewal times are in the

291   range 50-150 years and, as expected, increase to several centuries (and even

292   millenia) for the sites that show the highest dilution by old waters (Jannet, Hayet,

293   Sabrine, Marwa).

294   The discrepancy between tritium-based and F-12 / F-133-based renewal times

295   indicates that the well-mixed reservoir hypothesis is clearly oversimplified, thus

296   explaining why the renewal time is affected by the temporal shape of the tracer input

297   function. In actuality, the deep reservoirs are most likely characterized by vertical

298 gradients in tracer concentration. Therefore, analysing tracer concentrations at

299 various depth as well as monitoring tracer concentrations in the mineral waters as a

300 function of time would be very helpful to get a better view of the actual characteristics

301 of groundwater reservoir at each site.

302

303 **5. Conclusion**

304

305 We have analysed anthropogenic tracers (tritium/helium-3, SF_6, CFCs and

306 radiocarbon) in eleven mineral waters of northern and central Tunisia.

307 The analysis of the tracer results show that SF_6 and F-11 are not entirely reliable

308 due to an additional SF_6 component likely originating from in-situ production and a

309 slight but significant F-11 loss attributed to in-situ degradation. All carbon-14 values

310 are well below the natural modern value clearly showing the influence of the ^{14}C

311 dilution by dead Dissolved Inorganic Carbon. Therefore, the tracer analysis focussed

312 mainly on tritium, F-12 and F-113.

313 Tracer-tracer plots indicate that the analysed groundwaters are a mixture of

314 "modern" rainwater with older waters of pre-1950s ages, which constitute the main

315 groundwater reservoir. ^{14}C data suggest that the age of these old waters is of the

316 order of radiocarbon half-life or more.

317 The degree of dilution by these old waters is a qualitative indication of size of the

318 reservoir, and therefore of the sustainability of groundwater resource. More

319 quantitatively, the renewal time of each mineral groundwater was estimated using a

320 well-mixed reservoir hypothesis. Most of the studied sites have groundwater renewal

321 times in range from 50-150 years. For the sites where tracer concentrations are the

322 most diluted by old waters, this value increase to several centuries. However one

323 observes some serious discrepancies between tritium based and F-12 / F-133 based

324 results, clearly showing that the well-mixed reservoir hypothesis is oversimplified and

325 calling for additional tracer data and a better resolution of well screens to define the

326 vertical gradients in tracer concentration in the various reservoirs.

327

328 **6. Acknowledments**

329

330   The authors gratefully acknowledge the helpful contribution of the Office du

331 Thermalisme (Tunis). We also thank the director and technical staff of the mineral

332 water bottling plants for their kindness and assistance during sampling.

333

334 **Appendix A. Geological setting**

335
336   The Tunisian mineral waters are found in various geological domains, trapped in

337 the Jurassic, Upper Cretaceous and Eocene limestone reservoirs as well as the Mio-

338 Pliocene detrital reservoirs.

339   The Marwa mineral waters are captured by an inclined borehole, upstream of Ain

340 el Hammam natural spring. The latter was captured by the Romans via galleries. The

341 Upper Cretaceous fractured and karstified carbonate aquifer forms a large NE-SW

342 synclinal structure affected by faults in the same direction. The centre of the structure

343 is occupied by Paleocene marls providing partial protection of the aquifer against

344 pollution. The aquifer is supplied by infiltration of precipitation waters through

345 widespread carbonates outcropping and forming the Anntra and El Hara massifs.

346   Crystalline and Aqualine mineral waters are captured in the Jurassic limestones

347 by two deep drillings of 187 and 96 m respectively, both located to the NW side of the

348 Zaghouan massif. The waters are supplied by infiltration of precipitation in the

349   Zaghouan massif affected by numerous faults: the Zaghouan fault on the SE side

350   and by smaller faults on the NW side (Turki, 1985). The underground flows of

351   Jurassic aquifers waters are oriented towards the NW (mineral water catchment

352   area) and the SE of the Zaghouan massif (Zeriba thermal springs).

353   The Ain Garci mineral waters are captured by a gallery dug in the Eocene

354   limestones. They are probably mixed with the ascending waters of the upper

355   Cretaceous aquifers (Campanian and Cenomanian-Turonian limestones). The

356   physical-chemical characteristics of the mineral waters suggest a deep supply in

357   relation to volcanic rocks (basalt alkaline) associated with the Cenomanian-Turonian

358   carbonates recorded in Jebel Fadhloun and jebel Abid (Raaf and Althuis, 1952;

359   Laaridhi-Ouazaa, 1994). Ain Garci mineral waters show the highest radioactivity,

360   confirming the influence of volcanic rocks (Ben Belgacem, 2011).

361   The mineral water Safia (Ain Mizeb) is captured by a recent gallery in continuity

362   with a Roman gallery and also by drillings (Ain Ksiba). Ain Mizeb is located about 50

363   km south of El Kef and 800 m above sea level. The aquifer is housed in the Eocene

364   limestones of Sra Ouertène (Jellouli). It is a vast limestone plateau resting on the

365   phosphatic layers and covered in places by marls and lumachelles. This plateau is

366   affected by numerous faults and the source (Ain Mizeb) is associated with a fault

367   bringing the Eocene limestone sediments into contact with the marls. The drilling

368   (SO12) capturing Ain Ksiba is located on the edge of the collapsed part of the massif

369   of Sra Ouertene.

370   The mineral water Dima is recovered by a drilling upstream of the Ain M'rada at

371   the level of the wadi Lassoued syncline. This structure is formed by the Eocene

372   limestones and the central part is occupied by the Upper Eocene-Oligocene

373   sediments. It is affected by a series of oblique faults, the most important of which is

374 that of Ain Sassi. This structure constitutes an important hydraulic unit from which

375 emerges several sources: Ain Sassi, Ain Badi and Ain M'rada along the faults. The

376 Eocene limestones constitute the Dima mineral water aquifer. The direction flow of

377 groundwater is SW-NE, so water capture is located in the upstream part of the

378 aquifer.

379 Mineral waters of Fourat, Janet, Sabrine and Hayet are captured by drillings in the

380 Miocene detrital Formation: the water table of Janet aquifer is tapped by a 360 m

381 deep drilling intersecting the Mio-Pliocene detrital Formation near Haffouz (Kairouan)

382 which is in direct contact with Eocene limestone formations.

383 The Fourat mineral water comes from a source located at Ksar Lemsa in the

384 delegation of Oueslatia. The mineral water of Fourat is captured by a deep drilling

385 crossing the Mio-Pliocene formations which are in direct contact with the Eocene

386 limestone.

387 Sabrine waters are captured by a 154 m deep drilling in the southern part of the

388 Chougafia aquifer. It is trapped in a synclinal basin, the core of which is formed by

389 the Mio-Pliocene siliceous sands and is fed by the reliefs surrounding the structure.

390 The water flow of this aquifer is directed SW-NE (Farid et al., 2015) and the drilling,

391 collecting the mineral water is located in the upstream part of the aquifer.

392 Hayet mineral waters are captured by a 226 m deep drilling located at Baten El

393 Ghazel in the delegation of Jelma, 45 km away from Sidi Bouzid. The aquifer is

394 housed in the Miocene sandstone and sealed by marls. Water supply through

395 infiltration occurs throughout sandstones outcropping on the flanks of jebels Labeidh

396 and M'Rihla.

397

398 **7. References :**

399

400 Aeschbach-Hertig, W., Peeters, F., Beyerle, U., Kipfer, R., 1999. Interpretation of

401   dissolved atmospheric noble gases in natural waters. Water Resour. Res., 35,

402   2779-2792.

403 Ambach W, Dansgaard W, Eisner H, Mollner J., 1968. The altitude effect on the

404   isotopic composition of precipitation and glacier ice in the Alps: Tellus 20, 595-

405   600.

406 Ayraud, V., Aquilina, L., Labasque, T., Pauwels, H., Molenat, J., Pierson-Wickmann,

407   A.C., Durand, V., Bour, O., Tarits, C., Le Corre, P., Fourre, E., Mérot, P., Davy,

408   P., 2008. Compartmentalization of physical and chemical properties in hard rock

409   aquifers deduced from chemical and groundwater age analyses. Appl. Geochem.

410   23, 2686–2707.

411 Battle-Aguilar, J., Banks, E.W., Batelaan, O., Kipfer, R., Brennwald, M.S., Cook,

412   P.G., 2017. Groundwater residence time and aquifer recharge in multilayered

413   semi-confined and faulted aquifer systems using environmental tracers. J. Hydrol.

414   546, 150-165.

415 Baudron, P., Barbecot, F., Gillon, M., Arostegui, J.L.G., Travi, Y., Leduc, C., Gomariz

416   Castillo, F., Martinnez-Vicente, D., 2013. Assessing groundwater residence time

417   in a highly anthropized unconfined aquifer using bomb peak ^{14}C and

418   reconstructed irrigation [3]H. Radiocarbon 55, 993-1006.

419 Ben Belgacem, S., 2011. Les activités alpha et bêta globales dans l'eau minérale

420   tunisienne. PFE Chimie Industrielle INSA Tunis, 61 pp.

421 Beyerle, U., Aeschbach-Hertig, W., Hofer, M., Imboden, D.M., Baur, H., Kipfer, R.,

422   1999. Infiltration of river water to a shallow aquifer investigated with ^{3}H/^{3}He, noble

423   gases and CFCs. J. Hydrol. 220, 169–185.

424 Bullister, J.L., 2011. Atmospheric CFC-11, CFC-12, CFC-113, CCl4 and SF6

425   Histories.   http://cdiac.ornl.gov/ftp/oceans/CFC_ATM_Hist/.   Carbon   Dioxide

426   Information Analysis Center, Oak Ridge National Laboratory, US Department of

427   Energy, Oak Ridge, Tennessee.doi: 10.3334/CDIAC/otg.CFC_Hist.

428 Busenberg, E. and Plummer, N.L., 2000. Dating Young Groundwater with Sulfur

429   Hexafluoride: Natural and Anthropogenic Sources of Sulfur Hexafluoride, Water

430   Resour. Res. 36 (10), 3011-3030.

431 Busenberg, E., Plummer, L.N., 1992. Use of chlorofluorocarbons (CCl_3F and CCl_2F_2)

432   as hydrologic tracers and age dating tools: the alluvium and terrace system of

433   central Oklahoma. Water Resour. Res. 28, 2257–2283.

434 Busenberg, E., Plummer, L.N., 2000. Dating young groundwater with sulfur

435   hexafluoride: natural and anthropogenic sources of sulfur hexafluoride. Water

436   Resour. Res. 36, 3011–3030.

437 Celle-Jeanton, H., Zouari, K., Travi, Y., Daoud, A., 2001. Isotopic characterisation of

438   the precipitation in Tunisia. Variations of the stable isotope compositions of rainfall

439   events related to the origin of air masses. Compte-rendus de l'Académie des

440   Sciences, série IIa, 333, 625-631.

441 Clark, I. and Fritz, P., 1997. Environmental isotopes in hydrogeology. Lewis

442   Publishers, CRC Press, New York, 331pp.

443 Cook, P.G., Solomon, D.K., 1995. Transport of trace gases to the water table:

444   Implications for groundwater dating with chlorofluorocarbons and krypton-85.

445   Water Resour. Res. 31, 263–270.

446 Corcho Alvarado, J.A., Purtschert, R., Hinsby, K., Troldborg, L., Hofer, M., Kipfer, R.,

447   Aeschbach-Hertig, W., Arno-Synal H., 2005. ^{36}Cl in modern groundwater dated by

448   a multi-tracer approach (^{3}H/^{3}He, SF$_6$, CFC-12 and ^{85}Kr): a case study in

449   quaternary sand aquifers in the Odense Pilot River Basin, Denmark. Appl.

450   Geochem. 20, 599-609.

451 Corcho Alvarado, J.A., Purtschert, R., Barbecot, F., Chabault, C., Rueedi, J.,

452   Schneider, V., Aeschbach-Hertig, W., Kipfer, R. and Loosli, H. H., 2007.

453   Constraining the age distribution of highly mixed groundwater using ^{39}Ar: A

454   multiple environmental tracer (^{3}H/^{3}He, ^{85}Kr, ^{39}Ar and ^{14}C) study in the

455   semiconfined Fontainebleau Sands Aquifer (France). Water Resour. Res. 43,

456   W03427, doi:10.1029/2006WR005096.

457 Craig, H., 1961. Isotopic variation in meteoric water. Science 133, 1702-1703.

458 Darling, W.G., Gooddy D.C., MacDonald A.M., Morris B.L., 2012. The practicalities of

459   using CFCs and SF$_6$ for groundwater dating and tracing. Appl. Geochem. 27,

460   1688-1697.

461 Deeds, D.A., Vollmer, M.K., Kulongoski, J.T., Miller, B.R., Mühle, J., Harth, C.M.,

462   Izbicki, J.A., Hilton, D.R. and Weiss, R.F., 2008. Evidence for Crustal Degassing

463   of CF$_4$ and SF$_6$ in Mojave Desert Groundwaters, Geochim. Cosmochim. Acta 72,

464   999-1013.

465 Delbart, C., Barbecot, F., Valdes, D., Tognelli, A., Fourré, E., Purtschert, R.,

466   Couchoux, L., Jean-Baptiste, P., 2014. Investigation of young water inflow in karst

467   aquifers using SF_6–CFC–^{3}H/He–^{85}Kr–^{39}Ar and stable isotope components. Appl.

468   Geochem. 50, 164-176.

469   Farid, I., Zouari, K., Rigane, A., Beji, R., 2015. Origin of the groundwater salinity and

470   geochemical processes in detrital and carbonate aquifers: Case of Chougafiya

471   basin (Central Tunisia). J. Hydrol. 530, 508-532.

472   Fourré E., Di Napoli, R., Aiuppa, A., Parello, F., Gaubi, E., Jean-Baptiste, P., Allard,

473   P., Calabrese, S., Ben Mammou, A., 2011.Regional variations in the chemical and

474   helium-carbon isotope composition of geothermal waters across Tunisia.

475   Chemical Geology 288, 67-85.

476   Frija, A., Chebil, A., Speelman, S., Faysse, N., 2014. A critical assessment of

477   groundwater governance in Tunisia. Water Policy 16, 358-373.

478   Gat, J.R. and Carmi, I., 1970. Evolution of the isotopic composition of atmospheric

479   waters in Mediterranean Sea area, J. Geophys. Res. 75, 3039-3048.

480   Gooddy, D.C., Darling, W.G., Abesser, C., Lapworth, D.J., 2006. Using

481   chlorofluorocarbons (CFCs) and sulphur hexafluoride (SF_6) to characterise

482   groundwater movement and residence time in a lowland Chalk catchment. J.

483   Hydrol. 330, 44-52.

484   Harnisch, J. and Eisenhauer, A., 1998. Natural CF_4 and SF_6 on Earth. Geophys. Res.

485   Lett. 25 (13), 2401-2404.

486   Han, L.F., Plummer, L.N., 2016. A review of single-sample-based models and other

487   approaches for radiocarbon dating of dissolved inorganic carbon in groundwater.

488   Earth Science Reviews 152, 119-142.

489   Höhener, P., Werner, D., Balsiger, C., Pasteris, G., 2003. Worldwide occurrence and

490   fate of chlorofluorocarbons in groundwater. Water Resour. Res. 33, 1-33.

491   Jean-Baptiste, P., Mantisi, F., Dapoigny, A., Stievenard, M., 1992. Design and

492   performance of a mass spectrometric facility for measuring helium isotopes in

493   natural waters and for low-level tritium determination by the ^{3}He ingrowth method.

494   Int. J. Radiat. Appl. Instrum. 43, 881-891.

495   Jean-Baptiste, P., Fourré, E., Dapoigny, A., Baumier, D., Baglan, N., Alanic, G.,

496   2010. ^{3}He mass spectrometry for very low-level measurement of organic tritium

497   in environmental samples. J. Environ. Rad., 101, 185-190.

498   Kralik, M., Humer , F., Fank, J., Harum, T., Klammler, G., Gooddy, D., Sültenfuß, J.,

499   Gerber, C., Purtschert, R. 2014. Using ^{18}O/^{2}H, ^{3}H/^{3}He, ^{85}Kr and CFCs to

500   determine mean residence times and water origin in the Grazer and Leibnitzer

501   Feld groundwater bodies (Austria). Appl. Geochem. 50, 150-163.

502   Laaridhi-Ouazaa, N., 1994. Etude minéralogique et géochimique des épisodes

503   magmatiques mésozoïques et miocènes de la Tunisie. PhD Thesis, Univ. Tunis II,

504   457 pp.

505   Labasque, T., Ayraud, V., Aquilina, L., Le Corre, P., 2006. Dosage des composés

506   chlorofluorocarbonés et du tétrachlorure de carbone dans les eaux souterraines.

507   Application à la datation des eaux. Editions Géosciences Coll Cahiers

508   Techniques. ISBN:2-914375-38-7.

509   Lapworth, D.J., MacDonald, A.M., Krishan, G., Rao, M.S., Gooddy, D.C. and Darling,

510   W.G., 2015. Groundwater recharge and age-depth profiles of intensively exploited

511   groundwater resources in northwest India, Geophys. Res. Lett., 42, 7554–7562,

512   doi:10.100 2/2015GL0657 98.

513   Lucas, L.L., Unterweger, M.P., 2000. Comprehensive review and critical evaluation of

514   the half-life of tritium. J. Res. Natl. Inst. Stand. Technol. 105, 541-549.

515   Massmann, G., Sültenfuß, J.,Dünnbier, U., Knappe, A., Taute, T., Pekdeger, A.,

516   2008. Investigation of groundwater residence times during bank filtration in Berlin:

517   a multi-tracer approach. Hydrol. Process. 22, 788–801.

518   Mayer, A., Sültenfuß, J., Travi, Y., Rebeix, R., Purtschert, R., Claude, C., Le Gal La

519   Salle, C., Miche, H., Conchetto, E., 2014. A multi-tracer study of groundwater

520   origin and transit-time in the aquifers of the Venice region (Italy). Appl. Geochem.

521   50, 177-198.

522   Nydal, R., and K. Lövseth. 1996. Carbon-14 Measurements in Atmospheric CO_2 from

523   Northern and Southern Hemisphere Sites, 1962-1993. ORNL/CDIAC-93, NDP-

524   057. Carbon Dioxide Information Analysis Center, Oak Ridge National Laboratory,

525   Oak Ridge, Tennessee. 67 pp. doi: 10.3334/CDIAC/atg.ndp057

526   Oster, H., Sonntag, C., Munnich, K.O., 1996. Groundwater age dating with

527   chlorofluoro-carbons. Water Resour. Res. 32 (10), 2989-3001.

528   Plummer, L.N., Busenberg, E., Böhlke, J.K., Nelms, D.L., Michel, R.L., Schlosser, P.,

529   2001. Groundwater residence times in Shenandoah National Park, Blue Ridge

530   Mountains, Virginia, USA: a multi-tracer approach. Chemical Geology 179, 93-

531   111.

532   Plummer, L.N. and Glynn, P.D., 2013. Radiocarbon dating in groundwater systems.

533   In: Isotope methods for dating old groundwater, International Atomic Energy

534   Agency, Vienna, STI/PUB/1587, Chapter 4, 33-89.

535   Poreda, R.J., Cerling, T.E. and Solomon, D.K., 1988. Tritium and helium isotopes as

536   hydrologic tracers in a shallow unconfined aquifer. J. Hydrol., 103, 1-9.

537   Raaf, J.F.M. and Althuis, S.P., 1952. Présence d'ophites spilitiques dans le Crétacé

538   des environs d'Enfidaville. 19th International Geological Congress, Algiers, 2[d] Ser.

539   Tunisia 6, 127-137.

540   Schlosser, P., Stute, M., Dörr, H., Sonntag, C. and Münnich, K.O., 1988. Tritium/^{3}He

541   dating of shallow groundwater. Earth Planet. Sci. Lett., 89, 353-362.

542   Shapiro, S.D., Schlosser, P., Smethie, W.M., Stute, M., 1997. The use of H-3 and

543   tritiogenic He-3 to determine CFC degradation and vertical mixing rates in

544   Framvaren Fjord, Norway. Marine Chemistry 59 (1–2), 141-157.

545   Siegenthaler, U. and Oeschger, H., 1980. Correlation of ^{18}O in precipitation with

546   temperature and altitude, Nature 285, 314–317.

547   Solomon, D.K. and Sudicky, E.A., 1991. Tritium and helium-3 isotope ratios for direct

548   estimation of spatial variations in groundwater recharge. Water Resour. Res.,

549   27(9), 2309-2319.

550   Solomon, D.K., Schiff, S.L., Poreda, R.J. and Clarke, W.B., 1993. A validation of the

551   ^{3}H/^{3}He method for determining groundwater recharge. Water Resour. Res., 29(9),

552   2951-2962.

553   Solomon D.K., Genereux D.P., Plummer L.N., Busenberg E., 2010. Testing mixing

554   models of old and young groundwater in a tropical lowland rain forest with

555   environmental   tracers.   Water   Resour.   Res.   46,   W04518,

556   doi:10.1029/2009WR008341.

557   Stewart, M.K., 2012. A 40-year record of carbon-14 and tritium in the Christchurch

558   groundwater system, New Zealand: dating of young samples with carbon-14. J.

559   Hydrol. 430, 50-68.

560   Stute, M., Deák, J., Révész, K., Böhlke, J.K., Deseö, E., Weppernig, R., Schlosser,

561   P., 1997. Tritium/^{3}He dating of river infiltration: an example from the Danube in

562   the Szigetköz Area, Hungary. Groundwater 35 (5), 905–911.

563   Suckow, A., 2014. The age of groundwater – Definitions, models and why we do not

564   need this term. Appl. Geochem. 50, 222-230.

565   Szabo, Z., Rice, D.E., Plummer, L.N., Busenberg, E., Drenkard, S., Schlosser, P.,

566   1996. Age dating of shallow groundwater with chlorofluorocarbons, tritium/helium-

567   3, and flow path analysis, southern New Jersey coastal plain. Water Resour. Res.

568   32 (4), 1023–1038.

569   Thompson, G.M. and Hayes J.M., 1979. Trichloromethane in groundwater: A

570   possible tracer and indicator of groundwater age. Water Resour. Res., 15, 546-

571   554.

572   Turki M.M., 1985. Polycinématique et contrôle sédimentaire associé sur la cicatrice

573   Zaghouan- Nebhana. PhD Thesis, Univ. Tunis. C. ST-INRST Ed., 7, 252 pp.

574

575

576

577   **Figure captions**

578

579   Fig.1 : Map of Northern and Central Tunisia showing the location of the groundwater

580   sampling sites.

581

582   Fig.2 : Comparison of the stable isotopic composition of precipitation with the isotopic

583   composition of the groundwaters. Tunis and Sfax Local Meteoric Water Lines (dotted

584   lines) are from Celle-Jeanton et al. (2001). The Global Meteoric Water Line (GMWL)

585   and Mediterranean Meteoric Water Line (MMWL) are from Craig (1961) and Gat &

586   Carmi (1970), respectively.

587

588   Fig.3 : Tracer ages comparison : ^{3}H-^{3}He (light blue), F-11 (red), F-12 (yellow), F-113

589   (green), SF_6 (dark blue)

590

591   Fig.4 : Atmospheric concentration of the transient tracers for the northern hemisphere

592   as a function of time. CFC and SF_6 curves (a) are from Bullister (2011) and ^{14}C data

593   are from Nydal & Lövseth (1996). Tritium content of rainwater in Tunisia (b) was

594   constructed using all historical measurements from Central Mediterranean stations in

595   the   IAEA   Global   Network   of   Isotopes   in   Precipitation   database   (at

596   https://nucleus.iaea.org/wiser/gnip.php), including the times-series of tritium in

597   rainwater for Tunis and Sfax.

598

599   Fig.5 : CFC and SF_6 tracer plots showing F-113 versus F-12 (a), SF_6 versus F-12 (b)

600   and F-11 versus F-12 (c). The black and blue curves correspond to the PF model

601   and the PF model + dispersion respectively (see text). Numbers are travel times (in

602 year) in the PF model. The dotted line represents the mixing between a recharge

603 water of the year 2010 (upper right corner) and an old water endmember with zero

604 tracer concentration (lower left corner).

605

606 Fig.6 : (a) ^{3}H versus F-12. The black and blue curves correspond to the PF model

607 and the PF model + dispersion respectively (see text). Tritium values prior to 2010

608 are decay-corrected using a tritium half-life of 4500 d (Lucas and Unterweger, 2000).

609 Dotted curve represent mixing between old waters and a recharge water of the year

610 2010 . (b) ^{3}H versus ^{14}C (corrected for carbonate dissolution). NB: the initial ^{14}C value

611 of recharge waters, as given by the ^{14}C input function (Fig. 4a), can be modified by

612 interaction of infiltrating water with soil CO_2 from plant root respiration and microbial

613 degradation of soil organic matter. In semi-arid to arid environments however, those

614 biological interactions are minimal (Plummer and Glynn, 2013) so this effect is

615 neglected here.

616

617 Fig.7 : Comparison of the fraction of old water present at each site, estimated from

618 the F113 - F12 and tritium - F12 diagrams.

619

620

621 **Table captions**

622

623 Table 1 : Summary of the main relevant parameters for the sampled sites

624

625 Table 2 : Tracer results. CFCs and SF_6 tracer concentrations have been corrected

626 from excess air as defined by neon data and normalized to sea-level pressure and a

627 common temperature of 15°C to allow the comparison of all sites (note that the

628 uncertainty on CFC and SF_6 ages do not take into account the uncertainty on the air

629 excess correction, mostly because of the lack of knowledge of the exact recharge

630 altitude).

631

632 Table 3 : Estimated groundwater renewal time for the various sites based on tritium,

633 F-12 and F-113 data, assuming a well-mixed reservoir (see text).

Site	Geographic zone	Catchment type	Well depth (m)	Year of commissioning	Altitude of the site (m)	Average temperature (°C)		Average precipitation (mm)			Recharge temperature (°C) (precipitation weighed)	pH	HCO3 (mmol/l)
						January	July	January	July	Annual			
Marwa	Bizerte	well	72	1993	300	11,3	25,2	77	3	558	13,1	7,2	4,17
Safia (Ain Mizeb)	El Kef	surface	0	1968	880	7,1	26,5	65	9	509	12,9	7,3	3,87
Safia (Ain Ksiba)	El Kef	well	62	1992	900	7,1	26,5	65	9	509	12,7	7,0	3,71
Dima	El Kef	well	~50	2009	750	7,1	26,5	65	9	509	13,7	7,5	4,04
Cristaline	Zaghouan	well	187	2003	200	9,6	27,0	68	5	496	15,2	7,4	3,79
Aqualine	Zaghouan	well	96	2006	200	9,6	27,0	68	5	496	15,2	7,6	4,40
Ain Garci	Zaghouan	surface	0	1900	110	9,6	27,0	68	5	496	15,2	6,6	19,84
Sabrine	Kairouan	well	154	1991	106	11,7	29,1	23	5	306	17,6	7,5	3,80
Fourat	Kairouan	well	~150	2003	400	11,7	29,1	23	5	306	16,1	7,2	4,80
Hayet	Kairouan	well	226	1996	420	11,7	29,1	23	5	306	16,0	7,5	2,15
Jannet	Kairouan	well	360	2002	400	11,7	29,1	23	5	306	16,1	7,6	3,75

Table 1

Site	Tritium	Neon excess	3H-3He age	F-11	F-12	F-113	SF6	F-11 age	F-12 age	F-113 age	SF6 age	2-H	18-O	14-C	delta 13-C	14-C corrected
	(TU)	(%)	(year)	(pmol/L)	(pmol/L)	(pmol/L)	(pmol/L)	(year)	(year)	(year)	(year)			(pmC)	(permil)	(pmC)
Marwa (2009)	1,44 ± 0,13	230,1	34,6 ± 1,4											52,27 ± 0,21	-11,14	56,30
Marwa	1,35 ± 0,05	26,6	23,9 ± 0,6	0,69 ± 0,12	0,549 ± 0,07	0,081 ± 0,01	7,99E-04 ± 1,2E-04	42 ± 2	40 ± 3	32 ± 2	20 ± 2	-35,7	-6,45			
Safia-Ain Mizeb (2009)	3,29 ± 0,15	11,0	10,4 ± 2,4									-49,1	-7,84	55,07 ± 0,19	-11,82	55,90
Safia-Ain Ksiba	3,34 ± 0,06	7,3	9,98 ± 1,1	2,08 ± 0,12	1,320 ± 0,07	0,208 ± 0,01	1,27E-03 ± 1,2E-04	34 ± 2	31 ± 2	25 ± 2	13 ± 2	-49,9	-7,66	58,01 ± 0,22	-12,36	58,01
Dima	3,03 ± 0,08	50,1	12,9 ± 1,0	1,43 ± 0,12	1,067 ± 0,07	0,176 ± 0,01	1,33E-03 ± 1,2E-04	37 ± 2	34 ± 2	26 ± 2	12 ± 2	-50,5	-7,62	68,72 ± 0,24	-12,22	68,72
Cristaline	3,10 ± 0,08	34,5	19,8 ± 0,7	1,64 ± 0,12	1,134 ± 0,07	0,165 ± 0,01	1,66E-03 ± 1,2E-04	36 ± 2	33 ± 2	24 ± 2	8 ± 1	-36,3	-6,51	67,93 ± 0,24	-10,47	77,86
Aqualine	3,16 ± 0,12	31,1	19,5 ± 0,6	1,64 ± 0,12	1,069 ± 0,07	0,166 ± 0,01	1,73E-03 ± 1,2E-04	36 ± 2	34 ± 2	26 ± 2	7 ± 1	-36,0	-6,52	66,43 ± 0,21	-10,57	75,42
Ain Garci (2009)	0,49 ± 0,04	-0,4										-31,7	-5,65	2,25 ± 0,09	-0,75	36,00
Sabrine	0,23 ± 0,05	10,9	37,1 ± 1,7	0,14 ± 0,12	0,061 ± 0,07	0,034 ± 0,01	1,84E-04 ± 1,2E-04	51 ± 2	56 ± 3	37 ± 2	33 ± 2	-31,6	-5,26	31,30 ± 0,14	-8,50	44,19
Fourat	2,53 ± 0,05	8,2	26,8 ± 1,0	1,30 ± 0,12	0,894 ± 0,07	0,136 ± 0,01	1,20E-03 ± 1,2E-04	38 ± 2	36 ± 2	28 ± 2	14 ± 2	-38,8	-6,59	60,66 ± 0,20	-11,35	64,13
Hayet	0,10 ± 0,06	38,8	55,7 ± 17,7	0,25 ± 0,12	0,185 ± 0,07	0,031 ± 0,01	2,33E-04 ± 1,2E-04	48 ± 2	51 ± 3	43 ± 2	31 ± 2	-32,2	-5,10	34,54 ± 0,16	-10,94	37,89
Jannet	0,12 ± 0,07	16,3	48,1 ± 16,3	0,12 ± 0,12	0,045 ± 0,07	0,025 ± 0,01	3,02E-04 ± 1,2E-04	52 ± 2	58 ± 3	39 ± 2	29 ± 2	-37,2	-6,32	3,62 ± 0,10	-7,49	5,80

Table 2

Site	Tritium-based renewal time (yr)		F12-based renewal time (yr)		F113-based renewal time (yr)	
	w/r = 1	w/r = 10	w/r = 1	w/r = 10	w/r = 1	w/r = 10
Marwa	329	360	131	215	125	215
Safia-Ain Mizeb	108	n.a	-	-	-	-
Safia-Ain Ksiba	106	186	41	183	38	183
Dima	122	135	57	69	49	61
Cristaline	118	134	52	89	53	90
Aqualine	114	129	57	75	53	72
Ain Garci	950	n.a	-	-	-	-
Sabrine	2100	2100	1320	1390	320	400
Fourat	155	171	72	102	68	100
Hayet	4500	4500	430	470	350	400
Jannet	4100	4100	1800	1800	440	470

Table 3
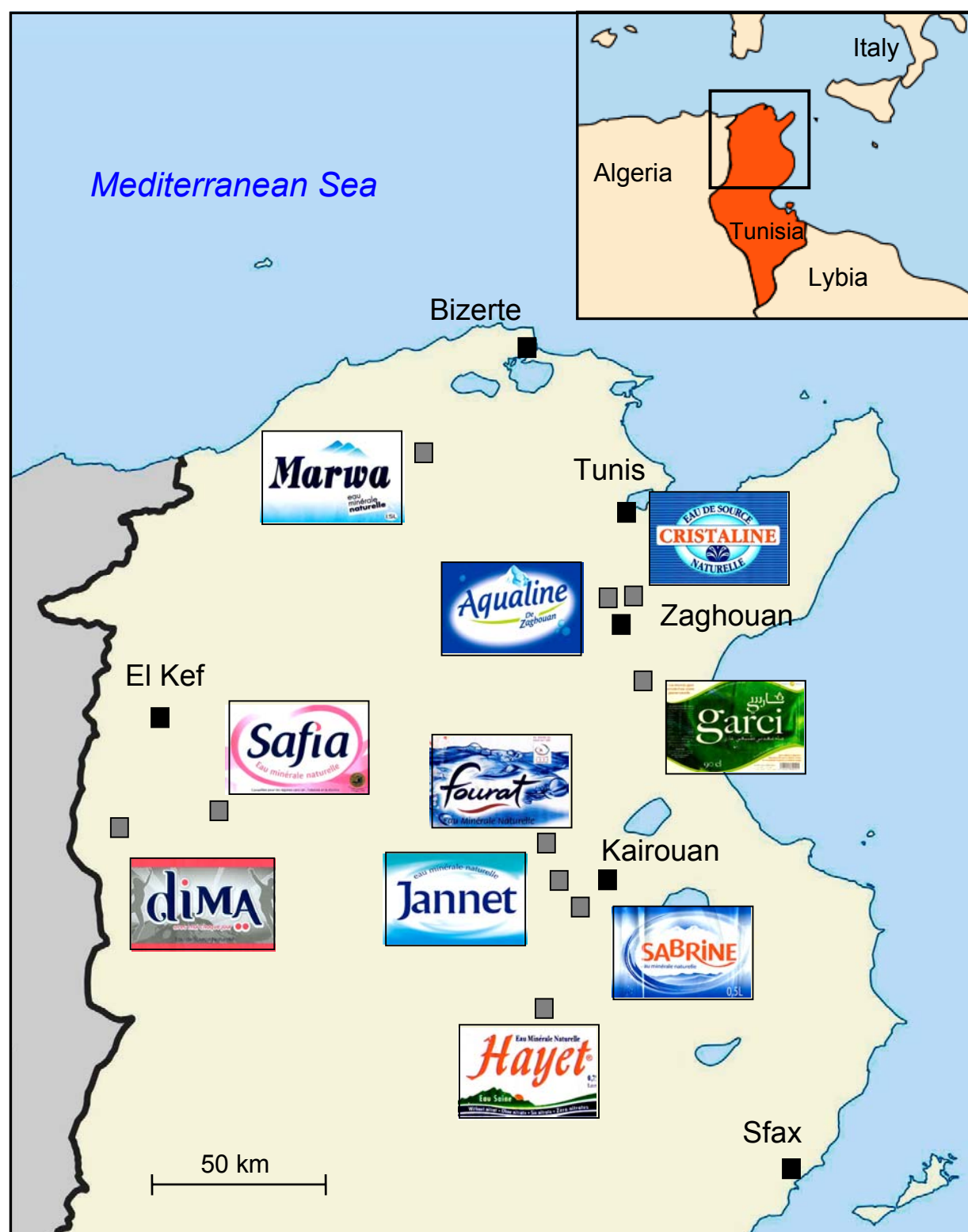
Figure 1
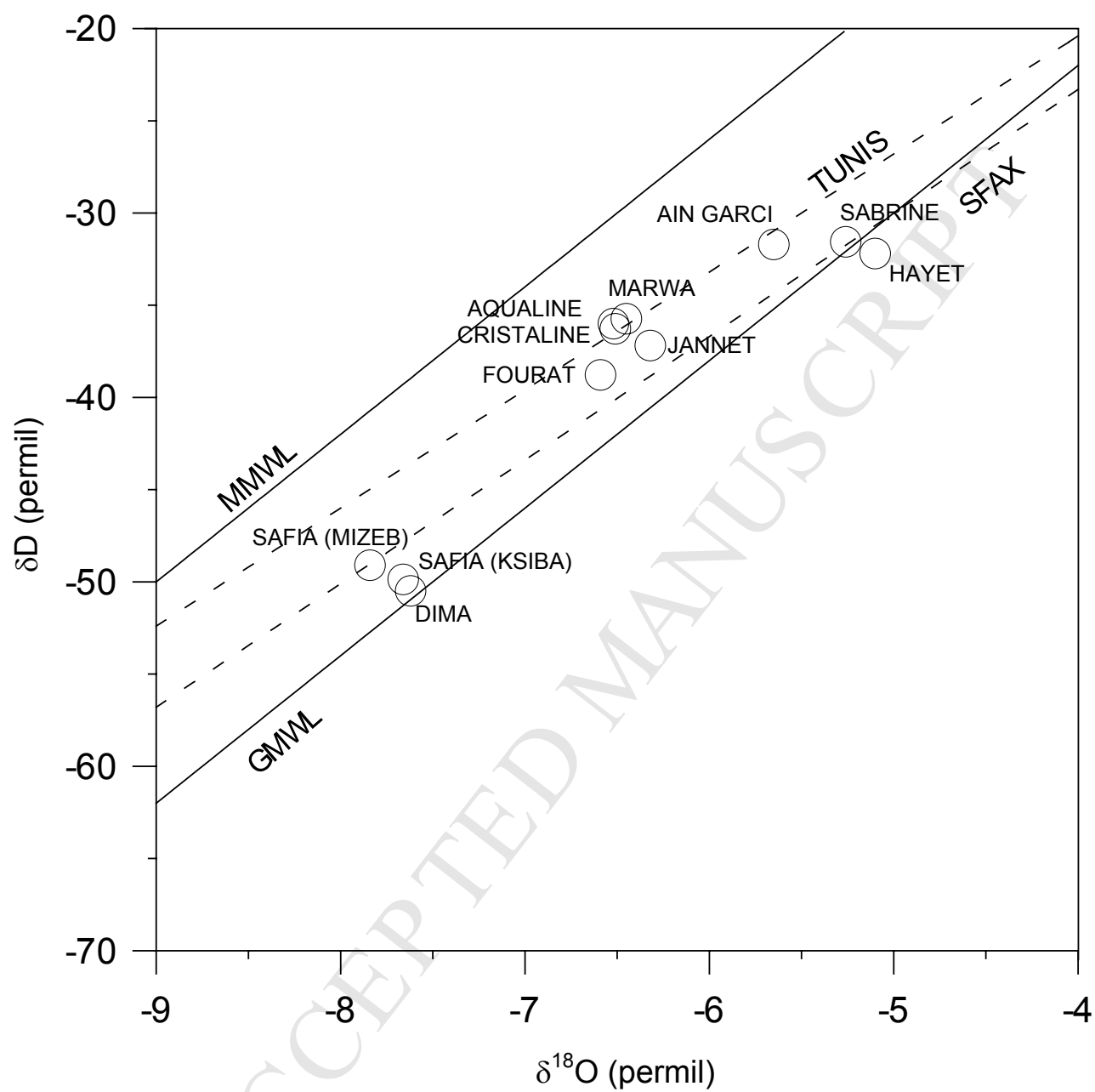
Figure 2
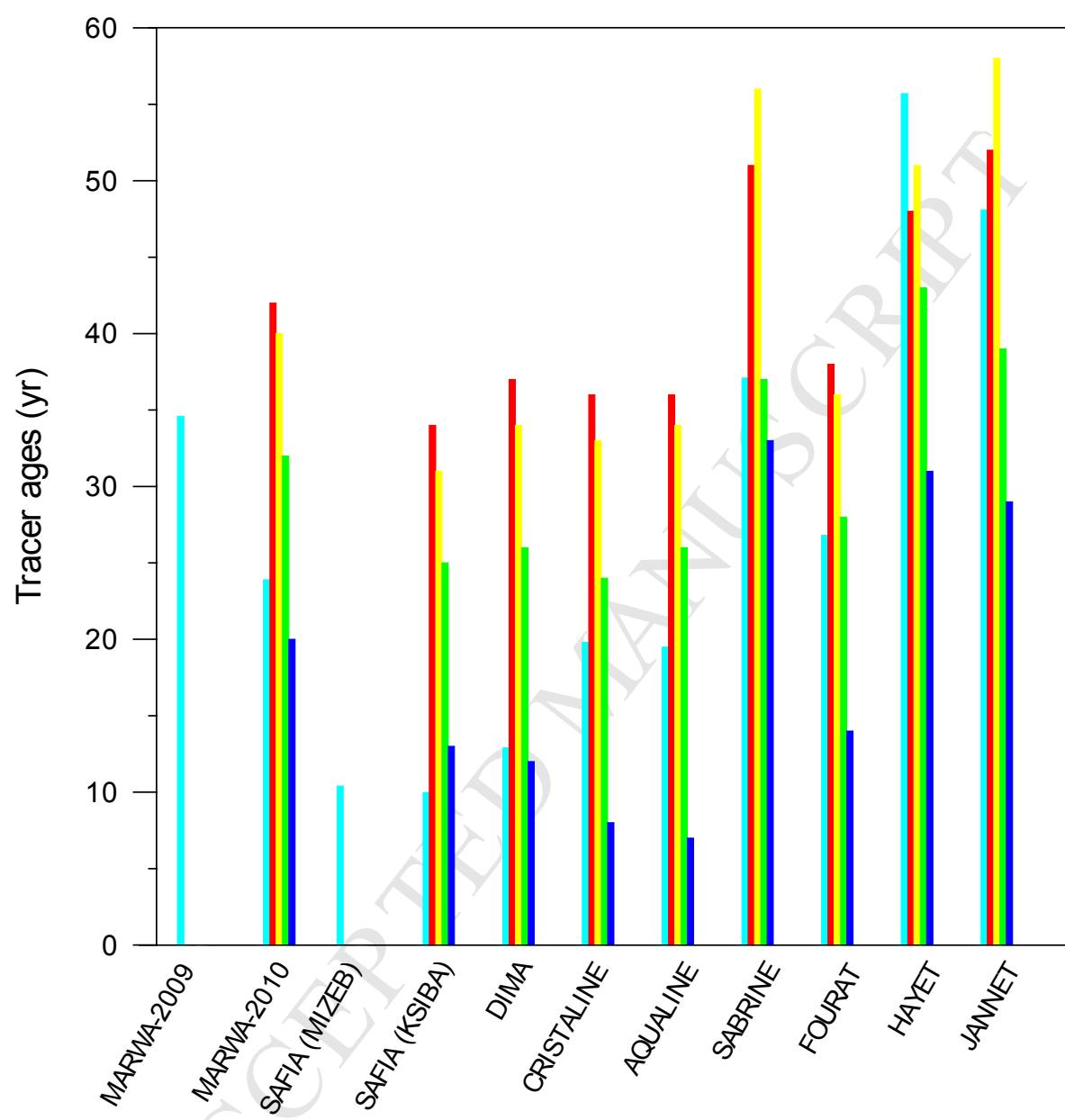
Figure 3
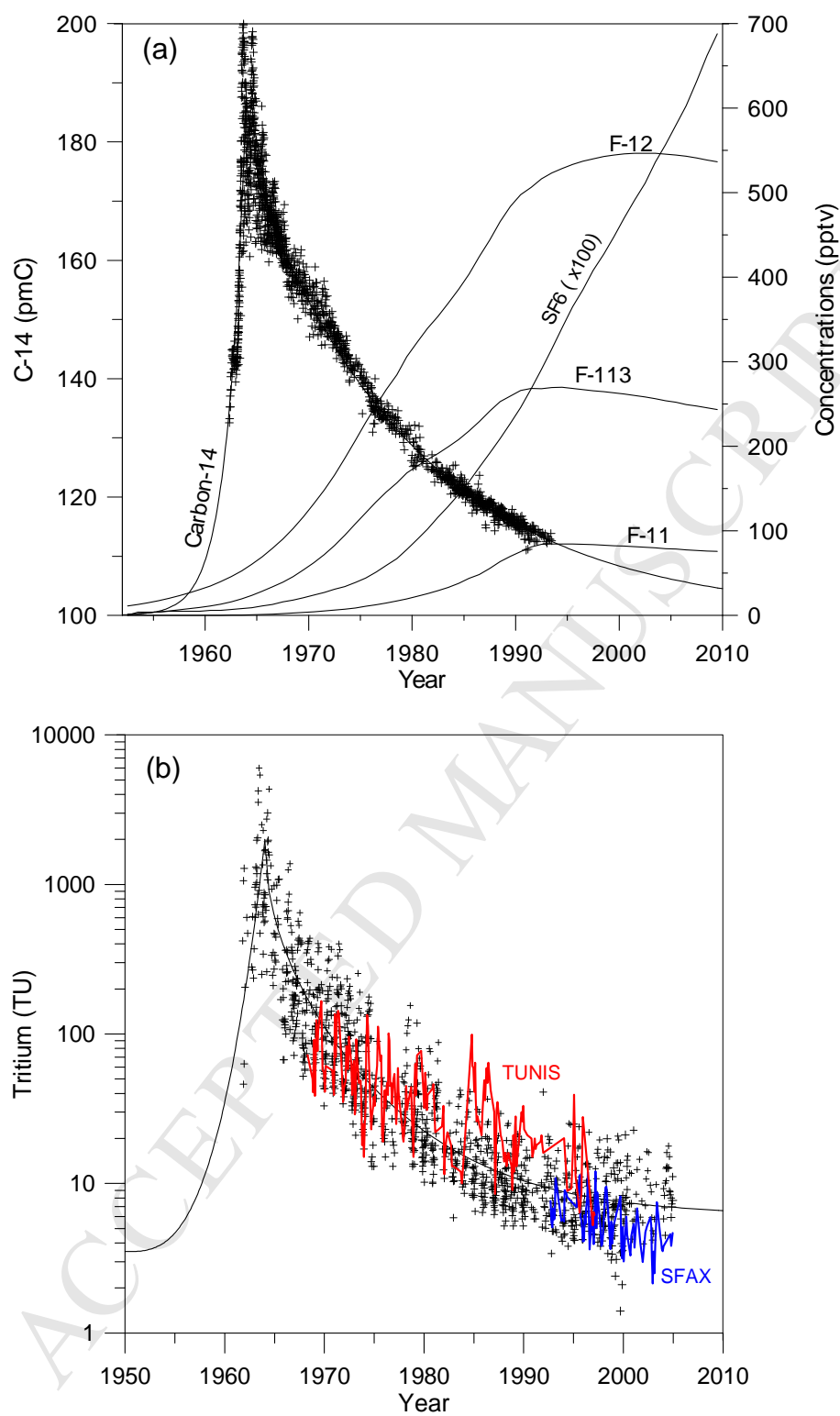
Figure 4
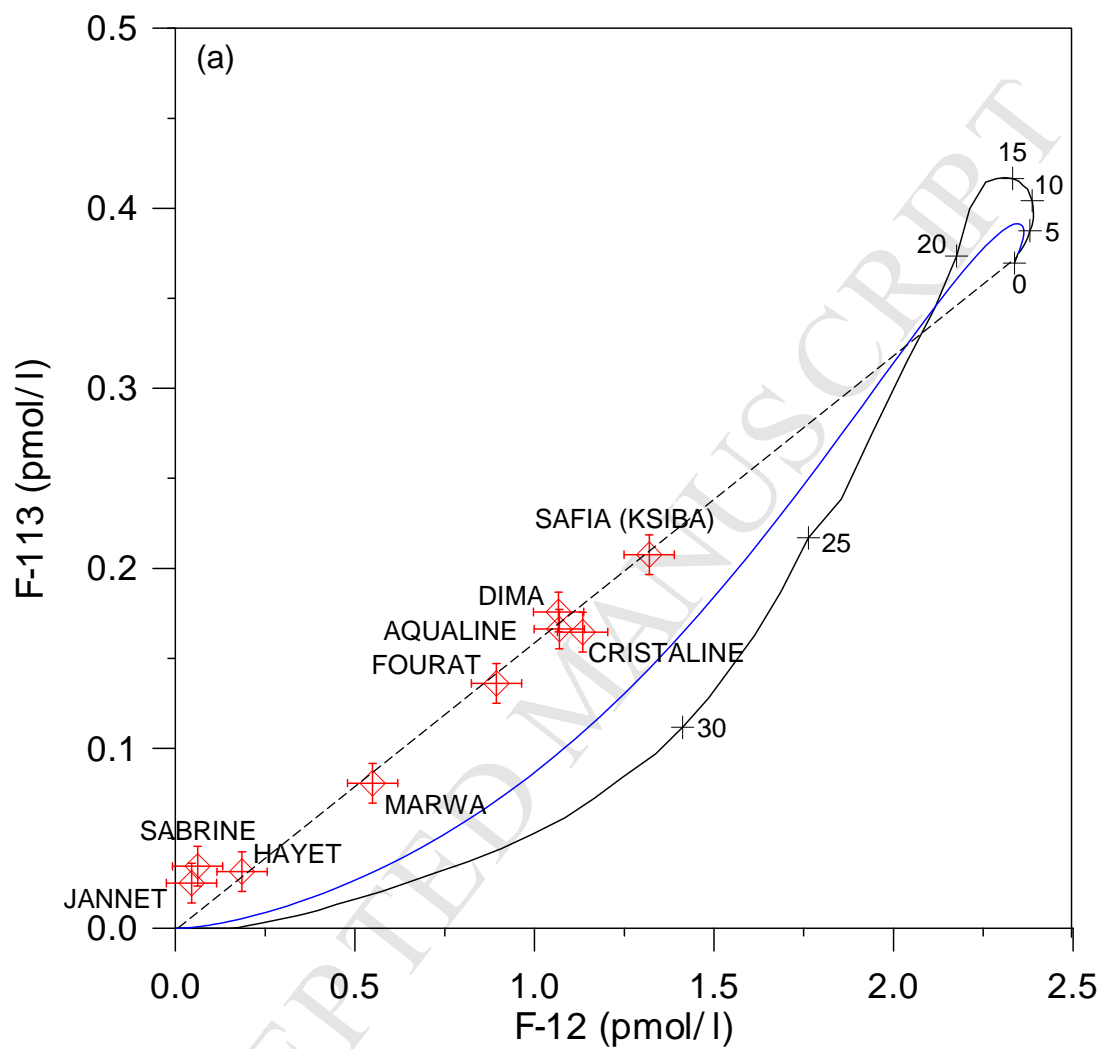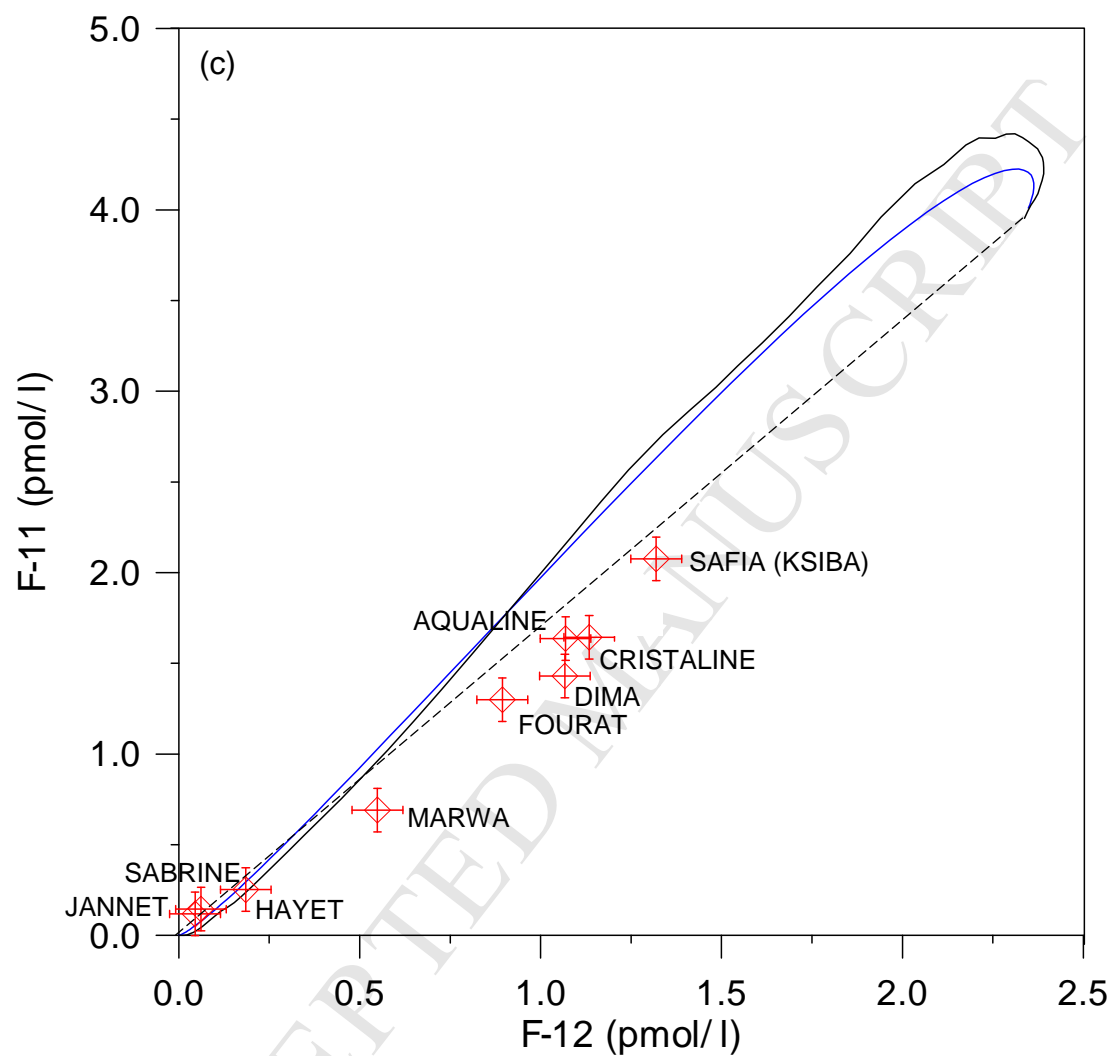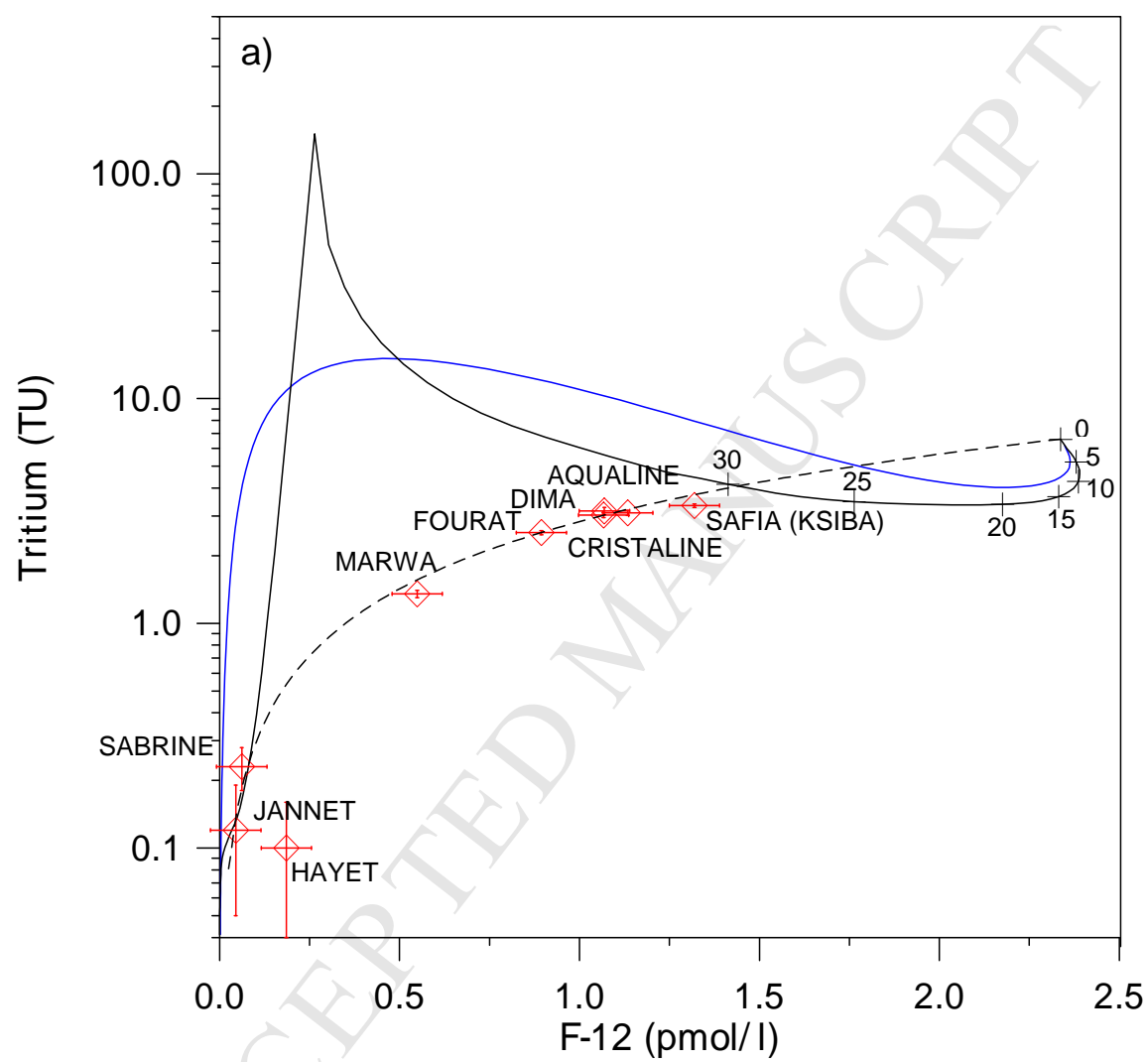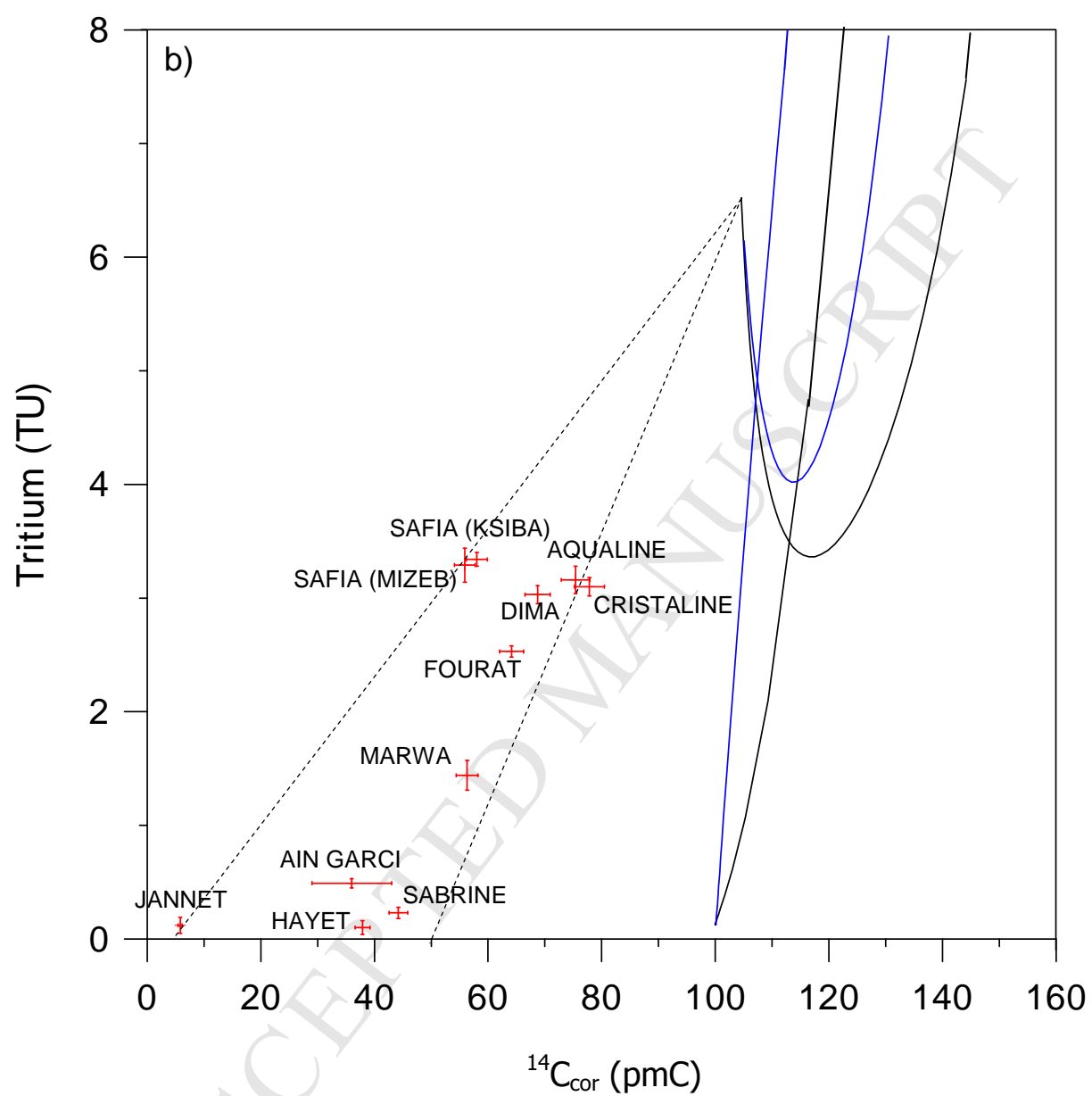
Figure 5a
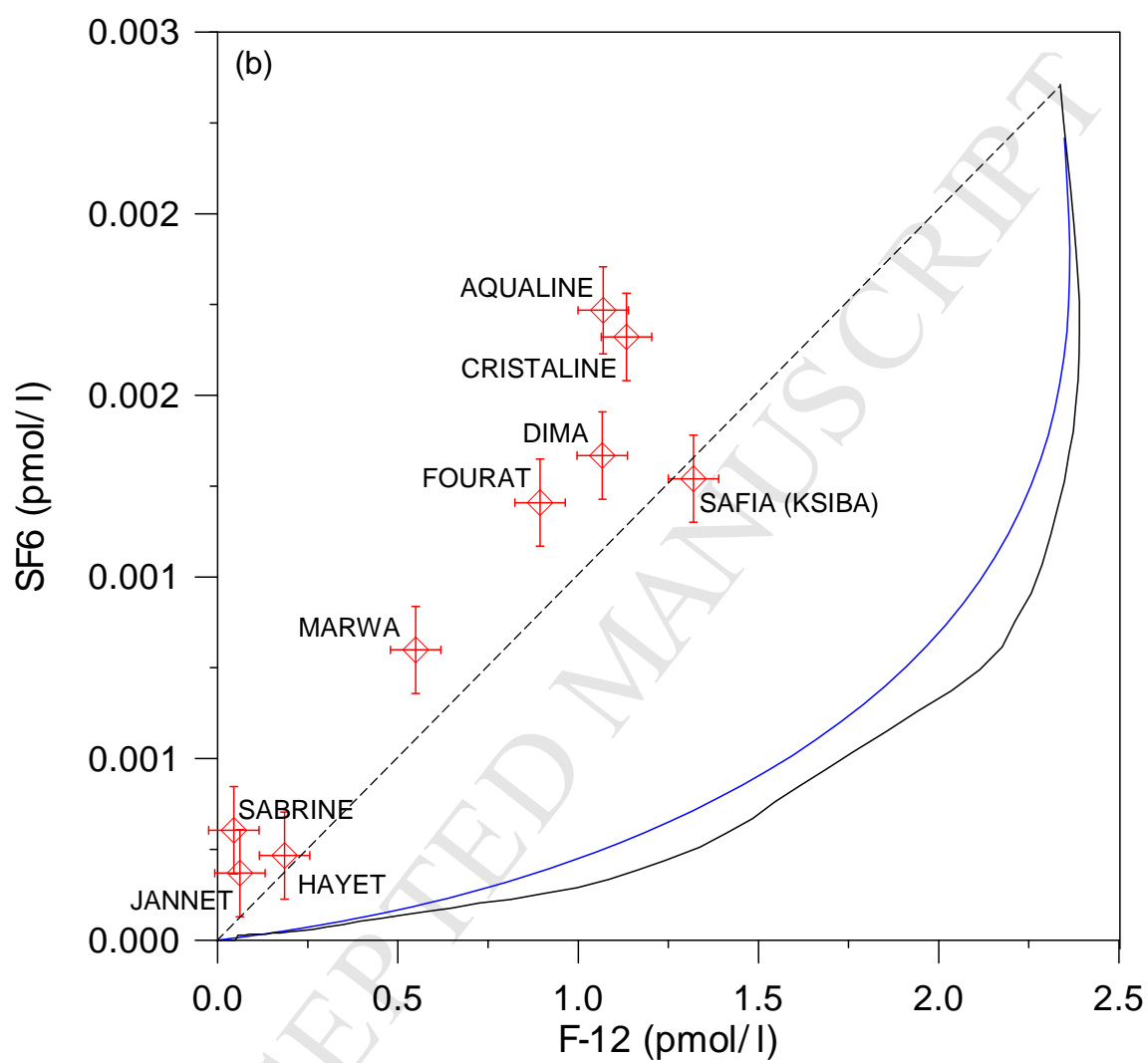
Figure 5b

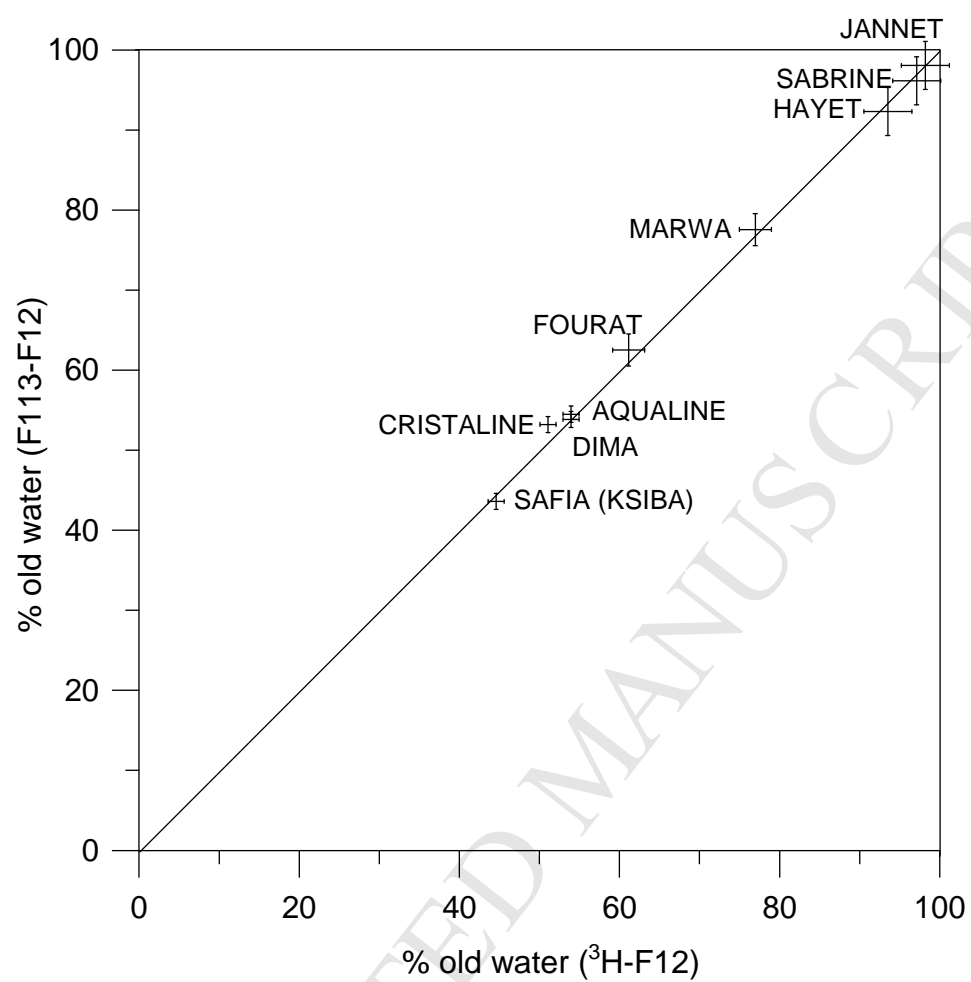Figure 5c

Figure 6a

Figure 6b

Figure 7

^{3}H-^{3}He, CFCs, SF$_6$ and ^{14}C were analyzed in commercial mineral groundwaters of Tunisia

All studied groundwaters are a mixture of modern rainwater with old groundwaters

Radiocarbon ages of these old groundwaters are in the range 5000-20000 years

Most groundwaters have renewal times between 50 years and several centuries